JTK: Jurnal Tadris Kimiya 11, 1 (June 2026): 94-111
Website: http://journal.uinsgd.ac.id/index.php/tadris-kimiya/index
ISSN 2527-9637 **(online) ISSN** 2527-6816 **(print)**

Green Synthesis of Gold Nanoparticles Using Red Ginger (Zingiber officinale Roscoe) Extract and CMC-Na as a Stabilizing Agent

Titta Hartyana Sutarna[1*], Hestiary Ratih[1], Arie Hardian[2,3] and Dwi Ayudhaningsih[1]
[1]Pharmacy Study Program, Faculty of Pharmacy, Universitas Jenderal Achmad Yani
[2]Study Program of Master of Chemistry, Fakultas Sains dan Informatika, Universitas Jenderal Achmad Yani
[3]Material and Environmental Development Center, Universitas Jenderal Achmad Yani
**E-mail: titta.hartyana@lecture.unjani.ac.id*

Received: May 2026; Accepted: June 2026; Published: June 2026

Abstract

Green synthesis of gold nanoparticles (AuNPs) using plant extracts has attracted increasing attention as an environmentally benign alternative to conventional chemical methods. However, achieving controlled particle size and long-term colloidal stability remains a significant challenge. This study investigated the potential of red ginger (Zingiber officinale Roscoe) rhizome extract as a bioreducing agent for gold-containing colloidal particle formation and evaluated the stabilizing effect of sodium carboxymethyl cellulose (CMC-Na). The extract was characterized through antioxidant and phytochemical analyses before being employed to reduce $HAuCl_4$. The resulting colloidal systems were analyzed using UV–Vis spectroscopy, polarized microscopy, particle size analysis, zeta potential measurement, and storage stability evaluation. The appearance of a purple-colored dispersion with surface plasmon resonance bands at 550–557.5 nm indicated the formation of gold-containing colloidal particles. Initial particle sizes ranged from 137 to 233.4 nm, with larger particles observed at higher extract concentrations, suggesting concentration-dependent particle growth or aggregation. Phytochemical constituents containing hydroxyl, carbonyl, and carboxyl functional groups are proposed to facilitate Au^{3+} reduction and contribute to the initial capping of the particles. Among the tested formulations, 2% CMC-Na provided the greatest improvement in short-term colloidal stability, delaying aggregation for approximately 14 days. Nevertheless, the substantial increase in hydrodynamic diameter during storage indicates the formation of aggregated or polymer-coated colloidal structures rather than well-dispersed AuNPs. These findings demonstrate the feasibility of red ginger extract for green gold colloid synthesis while highlighting the need for further optimization and advanced characterization to achieve smaller, more uniform, and long-term stable AuNPs.

Keywords: carboxy methyl cellulose sodium (CMC-Na), gold nanoparticles, red ginger rhizome (zingiber officinale Roscoe)

DOI: https://doi.org/10.15575/jtk.v11i1.55429

1. Introduction

Gold nanoparticles (AuNPs) are plasmonic nanomaterials with distinctive surface plasmon resonance (SPR) properties that make them attractive for sensing, imaging, diagnostic, and biomedical applications (Jain et al., 2006). Green synthesis offers an alternative route for preparing AuNPs by reducing the use of hazardous chemical reductants and organic solvents. In this approach, plant-derived metabolites can act as reducing and capping agents, making the process simpler, cost-

effective, and more environmentally friendly (Bharadwaj et al., 2021; Villagrán et al., 2024).

Recent studies have shown that plant-mediated green synthesis is a promising alternative for producing AuNPs because plant extracts contain diverse phytochemicals that can function as reducing, capping, and stabilizing agents (Fouda et al., 2022; Santhosh et al., 2022; Huq, 2025). Several recent reviews have emphasized the potential of plant-based AuNPs for biomedical, antimicrobial, antioxidant, catalytic, and sensing applications (Bharadwaj et al., 2021), (Muddapur et al., 2022), (Santhosh et al., 2022), (Huq, 2025), (Nisha et al., 2024). Similar green synthesis strategies have also been successfully applied to other metallic nanoparticles, including silver nanoparticles, demonstrating that phytochemicals from natural sources can serve as effective reducing agents for environmentally friendly nanoparticle production (Wahyudi et al., 2011). Despite these advantages, controlling particle size, polydispersity, surface chemistry, and long-term colloidal stability remains a major challenge because variations in phytochemical composition may lead to uncontrolled nucleation, particle growth, and aggregation during storage. Therefore, additional stabilizing agents, such as biocompatible polymers, are often required to improve colloidal stability.

Red ginger (*Zingiber officinale* Roscoe) rhizome was selected because it is a locally available medicinal plant rich in antioxidant secondary metabolites, including flavonoids, polyphenols, quinones, terpenoids, essential oils, gingerols, and shogaols (Shankar et al., 2004; Singh et al., 2008). These bioactive compounds may act as electron donors for the reduction of Au^{3+} ions and may also adsorb onto the particle surface as capping agents (Elia et al., 2014). Compared with many other plant extracts, red ginger is attractive because of its wide availability, low cost, and high antioxidant potential. Nevertheless, because the present study did not directly compare red ginger with other plant-derived reducing agents, its selection should be understood as a locally relevant and phytochemically promising choice rather than evidence of superior reducing performance. Similar antioxidant properties have also been reported in other Indonesian medicinal plants, such as gambir, whose high phenolic content contributes to strong free-radical scavenging activity (Aditya & Ariyanti, 2016). Likewise, numerous studies have demonstrated that phytochemical-rich plant extracts can simultaneously reduce metal ions and stabilize metallic nanoparticles, including silver nanoparticles, highlighting the broad applicability of plant-mediated green synthesis (Fabiani et al., 2018; Lembang, 2013; Thakkar et al., 2010)

Therefore, the use of a stabilizing polymer such as CMC-Na is expected to improve colloidal stability through steric and electrostatic stabilization (Tadros, 2007). However, the effectiveness of CMC-Na strongly depends on its concentration and interaction with the bioactive compounds present in the plant extract (Hebeish & Emam, 2010). Polymer-based nanoparticle systems have attracted considerable attention because polymer coatings not only improve colloidal stability but also enhance biocompatibility, surface functionality, and the potential for biomedical applications such as drug delivery and controlled release (DeFrates et al., 2018). This study evaluates the potential of red ginger rhizome extract as a bioreducing agent and CMC-Na as a stabilizer, with particular attention to the optical properties, particle size distribution, zeta potential, and storage stability of the resulting gold colloidal system.

Although several studies have reported the synthesis of AuNPs using plant extracts, limited attention has been given to the colloidal stability of red ginger-mediated AuNP systems after the addition of CMC-Na as a stabilizing polymer. In particular, the relationship between red ginger extract concentration, CMC-Na concentration, hydrodynamic particle size, zeta potential, and storage stability remains insufficiently discussed. Therefore, the novelty of this study lies in the preliminary evaluation of red ginger rhizome extract as a green reducing agent combined with CMC-Na as a polymeric stabilizer, with emphasis on the colloidal behavior and aggregation tendency

of the resulting gold-containing colloidal system.

2. Research Method

Red ginger rhizome was authenticated through macroscopic and microscopic observations, followed by standard simplicia characterization, including water content, total ash, water-soluble ash, acid-insoluble ash, and qualitative phytochemical screening. Phytochemical tests were conducted to identify major secondary metabolite groups, including flavonoids, polyphenols, alkaloids, quinones, saponins, tannins, steroids, and terpenoids, using standard colorimetric procedures. These analyses were performed to confirm the identity and phytochemical potential of the plant material as a source of reducing and capping compounds for gold colloid formation.

2.1. Macroscopic Testing

Macroscopic examination of red ginger rhizome was carried out visually to observe physical characteristics such as shape, color, odor, taste, and fiber appearance.

2.2. Microscopic Testing

Microscopic examination of red ginger rhizomes was performed using a microscope at appropriate magnification. This examination aimed to identify the characteristics and distinctive markers of red ginger rhizomes, such as starch grains, fiber bundles, and fibers.

2.3. Characterization of Red Ginger Rhizome (*Zingiber officinale* Roscoe) Simplex

Red ginger rhizome simplicia was characterized by determining water content, total ash, water-soluble ash, acid-insoluble ash, and phytochemical constituents.

2.3.1. Determination of Total Ash Content

The total ash content was determined by placing two grams of the crude drug into a previously heated and tared crucible. It was ignited on a stove until charred, then incinerated again in a furnace at 500°C, and finally cooled and weighed until it reached a constant weight. Consequently, the constant weight was the difference in weight between two consecutive weighings, each no more than 0.5 mg per gram of the remaining weight, and the test was carried out in duplicate.

2.3.2. Determination of Water-Soluble Ash Content

The determination of water-soluble ash content was carried out using the ash obtained from the total ash content determination. The ash was boiled in 25 mL of water for five minutes, then filtered using ash-free filter paper, washed with hot water, ignited for 15 minutes, and subsequently weighed. The analysis was conducted in duplicate.

2.3.3. Determination of Acid-Insoluble Ash Content

Acid-insoluble ash was determined using the total ash previously obtained. The ash was boiled with 25 mL of dilute hydrochloric acid for 5 min, filtered through ashless filter paper, washed thoroughly with hot water, ignited to constant weight, cooled in a desiccator, and weighed. The determination was performed in duplicate (WHO, 2011).

2.3.4. Determination of Water Content

Water content was determined using the azeotropic distillation method with water-saturated toluene. Approximately 5 g of powdered simplicia was transferred into a distillation flask, mixed with water-saturated toluene, and distilled using a Dean–Stark apparatus until no additional water was collected. After complete phase separation, the collected water volume was measured, and the moisture content was calculated based on the initial sample weight and expressed as percentage (v/w) (WHO, 2011).

2.3.5. Identification of Polyphenols

A 1-g sample was heated with water and filtered. Three drops of 1% iron(III) chloride solution were then added to the filtrate. The formation of a blackish-blue or green color indicated the presence of polyphenols (Harborne, 1998).

2.3.6. Identification the Flavonoids

1-gram of the sample was heated with water, then subsequently filtered. Additionally, 5 mL of the filtrate was transferred into a test tube, followed by the addition of magnesium powder and 1 mL of 2 N hydrochloric acid. the mixture was ignited in water, then filtered. The resulting filtrate was moved into another test tube, and 5 mL of amyl alcohol was added. Then, the mixture was shaken vigorously and allowed to stand until phase separation occurred. Consequently, the formation of a yellow-to-red color in the amyl alcohol layer indicated the presence of flavonoid compounds (Fransworth, 1996).

2.3.7. Identification the Tannins

One gram of powdered sample was extracted with distilled water by boiling for several minutes and filtered. A few drops of 1% gelatin solution were then added to the filtrate. The formation of a white precipitate indicated the presence of tannins (Evans, 2009).

2.3.8. Identification the Alkaloids

1-gram of the sample was triturated with 5 mL of dilute ammonia in a mortar, then 20 mL of chloroform was added while continuously grinding. Then, the mixture was filtered, and the chloroform layer was transferred into a test tube. Afterward, 5 mL of 2 N hydrochloric acid was added. Then, the mixture was vigorously shaken until two layers formed. The acid layer was separated and divided into three portions. The first portion was left blank. The second portion was treated with two until three drops of Mayer's reagent and observed for the formation of a white precipitate. The third portion was treated with two until three drops of Dragendorff reagent and observed for the formation of an orange-yellow to brick-red precipitate. These results indicated the presence of alkaloid compounds (Farnsworth, 1966).

2.3.9. Identification the Quinones

1-gram of the powdered simplicia was heated with water, and subsequently filtered. The filtrate was then treated with two until three drops of NaOH solution. The formation of a yellow-to-red color indicated the presence of quinone compounds in the sample (Farnsworth, 1966).

2.3.10. Identification the Saponins

2 grams of powdered simplicia were transferred into a test tube, and then 10 mL of hot water was added. The mixture was then cooled, vigorously shaken for 10 seconds, and treated with one drop of 2 N hydrochloric acid. The formation of a stable white foam 1–10 cm in height that persisted for at least 10 minutes indicated the presence of saponin compounds (Farnsworth, 1996).

2.3.11. Identification the Steroids and Triterpenoids

1-gram of powdered simplicia was triturated with 20 mL of ether, then filtered. The filtrate was evaporated to dryness using an evaporating dish. The residue was then treated with Liebermann–Burchard reagent. The formation of a purple color indicated the presence of terpenoid compounds, whereas the appearance of a green-blue color indicated the presence of steroid compounds (Farnsworth, 1966).

2.3.12. Identification the Monoterpenes and Sesquiterpenes

The powdered simplicia was triturated with ether, then pipetted and filtered. The filtrate was transferred into an evaporating dish and allowed to evaporate to dryness. The dried residue was subsequently treated with vanillin--SO_4 reagent. The formation of characteristic colors indicated the presence of monoterpenoid and sesquiterpene compounds (Harborne, 1987).

2.4. Preparation of Ethanolic Extract from Red Ginger Rhizome

In this step, red ginger rhizomes were cleaned from adhering impurities by washing under running water, cut into small pieces, and dried at 50°C. The dried material was subsequently ground using a blender and sieved through a 60-mesh sieve. red ginger was extracted using the maceration method. Then, 400 grams of finely powdered red ginger sample were macerated in 1.5 L of 96% ethanol for 3 × 24 hours, then filtered. The maceration process was repeated several times until a clear filtrate was obtained. The filtrate was then concentrated using a rotary evaporator at 40°C to obtain a viscous red ginger extract.

2.5. IC_{50} Determination of Red Ginger Rhizome Extract Using the DPPH Method

2.5.1. Preparation of DPPH reagent and red ginger extract test solutions

A stock solution of red ginger rhizome extract was prepared by dissolving 5 mg of concentrated extract in 100 mL of p.a. methanol. The stock solution was then diluted to obtain a concentration series of 5, 15, 20, 25, 30, and 35 ppm for the DPPH antioxidant assay. A total of 3 mL of each extract solution was mixed with 3 mL of DPPH solution, incubated for 30 minutes in the dark which was wrapped in aluminum foil to protect the DPPH solution from light, and measured at the maximum wavelength of DPPH. Each measurement was performed in triplicate (n = 3).

2.5.2. Preparation and Measurement of Red Ginger Rhizome Extract Test Solutions

Approximately 50 mg of red ginger rhizome extract was weighed, dissolved in 50 mL of p.a. methanol, and homogenized to prepare the stock solution. The stock solution was then diluted to obtain a series of test concentrations for the DPPH antioxidant assay. A total of 2 mL of each test solution was mixed with 2 mL of the previously prepared DPPH solution in a vial. The vial was wrapped with aluminum foil to protect the mixture from light and incubated for 30 minutes at room temperature. After incubation, the absorbance was measured using a UV-Vis spectrophotometer at the maximum wavelength of DPPH. All measurements were performed in triplicate (n = 3) (Munadi, 2020).

The percentage of inhibition was calculated using Equation 1.

$$\%\text{Inhibition} = \frac{A_{blank} - A_{sample}}{A_{blank}} \times 100\% \quad \text{(Equation 1)}$$

where A_blank is the absorbance of the DPPH blank solution and A_sample is the absorbance of the sample solution after reaction with DPPH.

A calibration curve was constructed by plotting the extract concentration against the percentage of inhibition. The linear regression equation was expressed as y = bx + a, where y represents the percentage of inhibition and x represents the extract concentration. The IC_{50} value was determined by substituting y = 50 into the regression equation and calculating the corresponding x value.

2.6. Preparation of Nominal 0.5 mM $HAuCl_4$ Solution

A total of 0.05 g of gold was dissolved in aqua regia prepared from HCl p.a. and HNO_3 at a 3:1 volume ratio (HCl:HNO_3). The dissolution was carried out under controlled heating until no metallic residue remained. The solution was then diluted to the mark with demineralized water in a 500 mL volumetric flask and homogenized. The prepared solution was used as a nominal 0.5 mM $HAuCl_4$ precursor solution.

2.7. Synthesis, Characterization, and Stabilization Study of Gold-Containing Colloidal Particles

Gold-containing colloidal particles were synthesized by mixing red ginger rhizome extract with 0.5 mM $HAuCl_4$ solution at an extract-to-$HAuCl_4$ volume ratio of 1:1. Red ginger extract concentrations of 600, 900, and 1,200 ppm were used for preliminary screening. The reaction mixture was protected from light and observed for color change from 1 to 24 hours as an initial indication of Au^{3+} reduction. For stabilization studies, CMC-Na was added at concentrations of 0.5%, 1%, and 2%, followed by mixing with $HAuCl_4$ solution under the same volume ratio. The resulting colloidal systems were characterized by UV-Vis spectroscopy, particle size analysis, zeta potential measurement, and storage stability evaluation.

2.7.1. Synthesis of Gold-Containing Colloidal Particles

A 10,000 ppm red ginger rhizome extract stock solution was prepared and diluted to the required concentrations. For each synthesis formulation, 5,000 µL of diluted red ginger rhizome extract solution was mixed with 5,000 µL of nominal 0.5 mM $HAuCl_4$ solution, resulting in an extract-to-$HAuCl_4$ volume ratio of 1:1. The mixture was placed in a microtube, protected from light using aluminum foil, and allowed to stand for 1–24 h to observe the formation of gold-containing colloidal particles. The formulation used in the stabilization study is presented in Table 1.

Table 1. Formulation of Gold-Containing Colloidal Particles Using Red Ginger Rhizome Extract and CMC-Na

Formula	Red Ginger Rhizome Extract Concentration (5000 µl)	$HAuCl_4$ Liquid Volume 0.5 mM	CMC-Na (Sodium Carboxymethyl Cellulose) Concentration (%)
F0	600 ppm	5,000 µl	-
F1	600 ppm	5,000 µl	0.5
F2	600 ppm	5,000 µl	1
F3	600 ppm	5,000 µl	2

In addition, the concentrations of red ginger rhizome extract used in this study, which are 600, 900, and 1,200 ppm, were selected as preliminary screening concentrations to evaluate the effect of extract concentration on the formation of gold-containing colloidal particles. This concentration corresponds to approximately 20 times the IC_{50} value and was assumed to provide sufficient antioxidant phytochemicals to support the reduction of Au^{3+} ions. The concentrations of 900 and 1,200 ppm were selected as stepwise increases to observe whether a higher amount of extract could improve the reduction process or instead increase organic capping, viscosity, and particle aggregation. Therefore, these concentrations were used for preliminary screening and should not be regarded as fully optimized synthesis conditions.

CMC-Na was added to the red ginger rhizome extract solution at concentrations of 0.5%, 1%, and 2%. The mixture was heated at 60°C for one minute to facilitate CMC-Na hydration and improve polymer dispersion in the extract solution. After heating, the mixture was allowed to cool to room temperature before the addition of 0.5 mM $HAuCl_4$ solution. Subsequently, the $HAuCl_4$ solution was added at an extract-to-$HAuCl_4$ volume ratio of 1:1, and the reaction mixture was protected from light using aluminum foil. The resulting colloidal system was then observed visually and characterized by UV-Vis spectroscopy, particle size analysis, and zeta potential measurement.

2.8. Characterization of Gold-Containing Colloidal Particles

Comprehensive characterization is essential in nanoparticle research because no single analytical technique can provide complete information regarding particle size, morphology, crystallinity, surface properties, and colloidal behavior. Therefore, multiple characterization methods are generally employed to obtain reliable nanoparticle data (Khairurrijal & Abdullah, 2009).

2.8.1. Visual observation

Visual observation of color change was conducted after 60 minutes and 24 h. A change in color from pale yellow or colorless to purple was used as a preliminary indication of gold-containing colloidal particle formation.

2.8.2. UV-Visible Spectrophotometry

The colloidal sample was placed in a cuvette and scanned using UV-Visible spectrophotometry in the visible region. The surface plasmon resonance band of AuNPs commonly appears in the range of approximately 500–600 nm, depending on particle size, shape, surface chemistry, and aggregation state.

2.8.3. Polarized Microscopy

Polarized microscopy was used as a supportive observation to evaluate the possible presence of microscale residues or aggregates in the dried colloidal sample. The sample was placed on a glass slide, and the solvent was allowed to evaporate before observation.

2.8.4. Particle Size Measurement by PSA/DLS

Particle size analysis is an important characterization technique because it provides information regarding particle size distribution and homogeneity. Reliable particle size determination requires proper instrument performance and standardized measurement conditions (Nuraeni et al., 2013). Since particle size strongly influences colloidal stability and nanoparticle performance, PSA/DLS was employed in this study to evaluate the synthesized colloidal particles (Tarhan et al., 2019). Two to three drops of the sample were dispersed in demineralized water in a cuvette and then placed in the instrument holder for particle size measurement by PSA/DLS.

2.8.5. Zeta Potential Measurement

For zeta potential measurement, 10 drops of the sample were diluted in 10 mL of demineralized water. The diluted sample was transferred into a zeta cell using a syringe and analyzed using the zeta potential mode of the instrument.

2.8.6. Storage Stability Evaluation

Storage stability of the CMC-Na-containing colloidal systems was evaluated by monitoring visual appearance, UV-Visible spectra, particle size, PDI, and zeta potential at selected storage times.

3. Result and Discussion

The first step before forming gold nanoparticles was identifying the red ginger rhizome, which included macroscopic and microscopic testing. The results of the macroscopic testing are shown in Table 2.

Table 2. Macroscopic Characteristics of Red Ginger Rhizome

Inspection Parameters	Result
Slice shape	Oval shape, yellowish white color
Color	The outer color is red and the flesh is yellowish white
Smell	Typical ginger and pungent
Flavor	Spicy
Fiber free	Contains free fiber
Intact/Break-free	There are protruding fibers

Furthermore, a microscopic examination of the red ginger rhizome was performed. This test aimed to identify whether the plant used was indeed red ginger rhizome. The results can be seen in Figure 1.

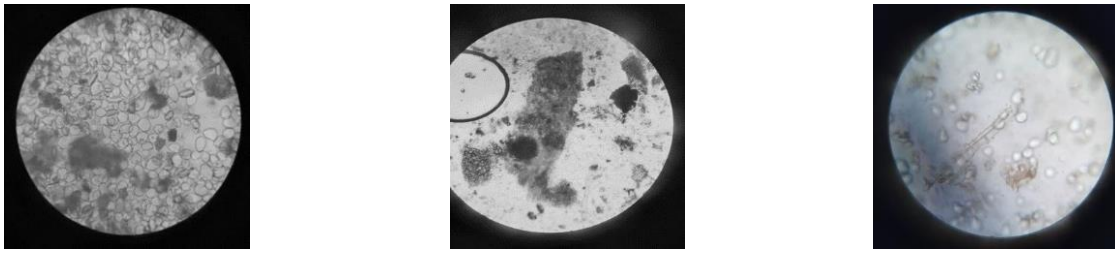

a b c

Figure 1. Microscopic Characteristics of Red Ginger Rhizome (Zingiber Officinale Roscoe): (A) Starch Granules, (B) Fiber Bundles, and (C) Fibers.

After the microscopic examination, the water and ash contents of the crude drug were determined. The purpose of the red ginger rhizome sample water content test was to determine its water content. This test was performed to prevent the growth of microorganisms during sample storage. The water content test results were 3.1% ± 2.35%. This result meets the requirements of the Indonesian Herbal Pharmacopeia, which specifies a water content of less than 10%.

The ash content test consisted of total ash content, water-soluble ash content, and acid-insoluble ash content. The ash content test result was 5.1%. The water-soluble ash test was then performed: the total ash content was obtained, then the residue was boiled in 25 mL of water for 5 minutes and filtered through ash-free filter paper. The water-soluble ash content result was 4.9%. The results of the ash content determination in red ginger rhizomes are listed in Table 3.

Table 3. Ash Content of Red Ginger Rhizome Simplicia

Types of Characterization	Ash Content Determination Results
Total Ash Content	4.9% ± 0.12
Water Soluble Ash Content	4.6% ± 0.32
Acid Insoluble Ash Content	1.81% ± 0.35

The phytochemical screening results (Table 4) indicate the presence of alkaloids, polyphenols, flavonoids, quinones, and triterpenoids in red ginger rhizome extract. These compounds may contribute to the reduction of Au^{3+} ions and the stabilization of the formed colloidal particles through electron donation and adsorption of functional groups on the particle surface. However, because the present study only performed qualitative phytochemical screening, the exact contribution of each metabolite group cannot be determined. Quantitative analyses such as total phenolic content and total flavonoid content are needed to correlate the reducing ability of the extract with its phytochemical composition. Therefore, the proposed role of flavonoids and other secondary metabolites as reducing and capping agents should be regarded as a possible mechanism rather than a confirmed mechanism.

Table 4. Phytochemical Screening Results of Red Ginger Rhizome Extract

Secondary Metabolites	Result	Description
Alkaloid	+	Detected
Polyphenols	+	Detected
Tannin	-	Not detected
Flavonoid	+	Detected
Quinone	+	Detected
Saponin	-	Not detected
Monoterpenoid	-	Not detected
Triterpenoid	+	Detected

Red ginger rhizome extract was obtained by maceration with 96% ethanol. The maceration method was chosen for its simple procedure and minimal equipment requirements. It did not require heating, thus preventing decomposition of the sample or plant. In addition, cold extraction yielded a higher extract. Moreover, 96% ethanol was an ideal solvent for preliminary extraction due to its ability to extract a wide range of compounds, from nonpolar to polar. The extraction method and solvent selection greatly influence the composition of phytochemical constituents obtained from medicinal plants because compounds differ in polarity and extraction efficiency. Therefore, extraction conditions should be carefully selected according to the intended biological activity (Tetti, 2014).

We used 96% ethanol as a solvent, which preferentially extracts polar antioxidant compounds. The extract was evaporated to obtain a thick extract. The resulting thick red ginger extract weighed 201 grams, yielding 22.33%. This demonstrates compliance with the Indonesian Herbal Pharmacopeia, Edition II, which requires a red ginger rhizome extract yield of at least 17.0%.

The next step was to test the antioxidant activity of the concentrated red ginger rhizome extract. Antioxidant activity testing of the ethanol extract of red ginger rhizome was performed using the DPPH (2,2-diphenyl-1-picrylhydrazyl) method. This method was simple, highly sensitive to free radicals, and fast, requiring only a small sample to evaluate the antioxidant activity of natural compounds. Additionally, the sample's antioxidant activity caused a color change in the DPPH solution in methanol, from purple to a slightly yellowish hue. This produced a change in absorbance at the DPPH maximum wavelength, measured with a UV-Vis spectrophotometer, thereby determining antioxidant activity (Molyneux, 2004).

Red ginger rhizome contains secondary metabolites, including flavonoids and polyphenols. These compounds may donate hydrogen atoms or electrons to DPPH radicals, thereby stabilizing the radical species and decreasing absorbance at the DPPH maximum wavelength. In this study, the maximum absorbance of DPPH was observed at 516 nm.

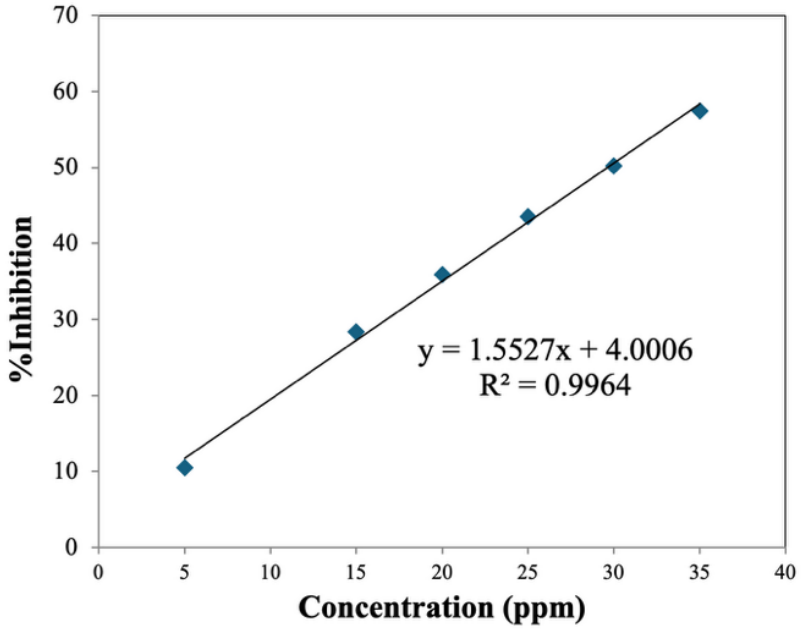

Figure 2. DPPH Radical-Scavenging Activity of Red Ginger Rhizome Extract, Showing The Relationship Between Extract Concentration and Inhibition Percentage

The DPPH antioxidant activity of red ginger rhizome extract was evaluated by plotting extract concentration against inhibition percentage, as shown in Figure 2. The linear regression equation was y = 1.5527x + 4.0006 with an R^2 value of 0.9964, indicating good linearity within the tested concentration range. The IC_{50} value was calculated by substituting y = 50 into the regression equation, resulting in an IC_{50} value of 29.63 µg/mL.

The IC_{50} value of red ginger rhizome extract obtained in this study was 29.63 µg/mL, indicating strong DPPH radical scavenging activity under the tested conditions. This value is lower than the IC_{50} value of 46.91 ppm reported for 96% ethanol extract of red ginger rhizome (Dewi et al., 2024) and also lower than the IC_{50} value of 46.12 ppm reported for red ginger powder without sucrose (Kamaluddin et al., 2024). These differences may be attributed to variation in plant origin, extraction solvent, extract concentration, sample preparation, and DPPH assay conditions. Comparable antioxidant activity of red ginger has also been reported using the DPPH method, although differences in extraction procedures and plant origin may lead to variations in IC_{50} values among studies (Yuliani et al., 2016). The relationship between phenolic compounds and antioxidant activity has also been reported in other medicinal plants, where higher phenolic content generally resulted in stronger free radical scavenging capacity (Khairun & Desty, 2018). Recent studies on 96% ethanol extract of red ginger have likewise reported high antioxidant activity, confirming that ethanol is an effective solvent for extracting antioxidant compounds from red ginger rhizomes (Dewi et al., 2024). Therefore, although the IC_{50} result supports the antioxidant potential of red ginger rhizome extract, it should be interpreted cautiously because the present study did not include a positive control such as ascorbic acid, gallic acid, Trolox, or quercetin. Further analysis of total phenolic and flavonoid contents would also be useful to correlate antioxidant capacity with the reducing ability of the extract toward Au^{3+} ions.

A limitation of the present antioxidant assay is the absence of a positive control, such as ascorbic acid, gallic acid, or Trolox. Therefore, the IC_{50} value obtained for red ginger rhizome extract should be interpreted as a descriptive estimate of its DPPH radical scavenging activity under the experimental conditions rather than as a benchmarked antioxidant performance. Future studies should include a standard antioxidant as a positive control to validate and compare the antioxidant capacity of the extract more rigorously.

To form gold nanoparticles, a 0.5 mM $HAuCl_4$ solution was prepared by dissolving gold in aqua regia. Aqua regia was made by mixing HNO_3 and HCl in a 3:1 ratio and heating until gaseous explosions occur. Aqua regia was used to dissolve gold because it was a strong acid capable of dissolving metal compounds (Amiruddin & Taufikurohmah, 2013). In this study, the final Au^{3+} concentration was not independently verified by analytical methods such as AAS or ICP-OES. Therefore, the reported concentration should be interpreted as the nominal precursor concentration.

The nominal $HAuCl_4$ solution was diluted with deionized water before use. Deionized water was selected to minimize interference from other dissolved metal ions. UV-Vis observation in the 200–400 nm range was used only as a preliminary check of the precursor solution and not as quantitative verification of Au^{3+} concentration.

Nanoparticles were produced using red ginger rhizome extract at three concentrations. These variations were selected based on previous research and were also influenced by the plant's IC_{50} value. The lowest concentrations used were 600, 900, and 1200 ppm. the mixing process was carried out at room temperature and protected from light. This was to prevent oxidation of the $HAuCl_4$ solution by the light, which could affect the formation of gold nanoparticles.

A color change from pale yellow or colorless to purple was used as a preliminary visual indication of gold-containing colloidal particle formation. This observation was recorded for all extract concentrations from 60 minutes to 24 h.

UV-Vis spectroscopy was then used to evaluate the optical response of the colloidal systems. In general, AuNP-containing colloids exhibit SPR absorption in the visible region, commonly around 500–600 nm, depending on particle size, shape, surface chemistry, and aggregation state (Taufikurohmah et al., 2012).

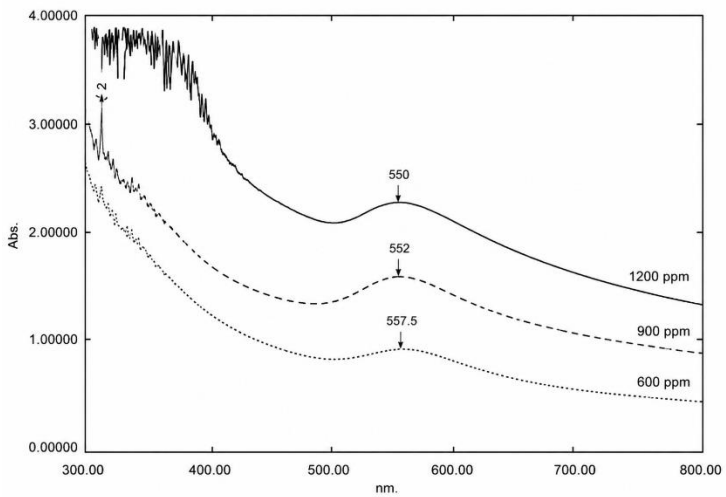

Figure 3. UV-Vis Absorption Spectra of Gold-Containing Colloidal Particles Synthesized Using Different Red Ginger Extract Concentrations

The absorption spectra in Figure 3 show SPR bands at 557.5, 552, and 550 nm for samples prepared with 600, 900, and 1,200 ppm red ginger extract, respectively. The slight blue shift with increasing extract concentration suggests changes in SPR behavior, possibly related to phytochemical capping and the local dielectric environment. However, this shift does not directly confirm a decrease in particle size because the PSA/DLS data showed larger hydrodynamic diameters at higher extract concentrations. Therefore, the UV-Vis results should be interpreted as preliminary optical evidence for gold-containing colloidal particle formation.

The colloidal particles were further characterized by PSA/DLS to determine their hydrodynamic size distribution. PSA/DLS measures the hydrodynamic diameter of particles undergoing Brownian motion; therefore, the measured size may include the metallic core, phytochemical capping layer, solvation shell, and possible aggregates. The hydrodynamic sizes were 137 nm, 208.4 nm, and 233.4 nm for samples prepared with 600, 900, and 1,200 ppm extract, respectively. The apparent inconsistency between the UV-Vis blue shift and increasing PSA/DLS size may arise because UV-Vis reflects plasmonic behavior, whereas PSA/DLS reports hydrodynamic diameter. Thus, the two techniques should be interpreted as complementary rather than direct measurements of the same particle dimension.

The increase in particle size with increasing red ginger rhizome extract concentration can be interpreted using the nucleation-growth concept. At 600 ppm, the amount of reducing phytochemicals may be sufficient to reduce Au^{3+} ions and promote the formation of relatively smaller colloidal particles. However, at higher extract concentrations of 900 and

1200 ppm, the increased amount of reducing agents may accelerate the reduction process and promote rapid particle growth. In addition, excess organic compounds from the extract may form thicker capping layers around the particles or promote interparticle interactions, resulting in larger hydrodynamic diameters. Therefore, the increase in particle size at higher extract concentrations suggests that excessive bioreductant does not necessarily improve particle size control and may instead promote growth and aggregation of the colloidal particles.

The color change from pale yellow/colorless to purple and the appearance of absorption bands at 550–557.5 nm indicate the formation of gold-containing colloidal particles through the reduction of Au(III) ions by phytochemical compounds present in red ginger rhizome extract. However, particle size analysis showed relatively large hydrodynamic diameters, particularly after the addition of CMC-Na, suggesting that the formed particles were not fully dispersed as small AuNPs but tended to form aggregated or polymer-coated colloidal structures. Therefore, the UV-Vis results should be interpreted as evidence of AuNP formation, while the PSA results indicate that further optimization is still required to control particle growth and aggregation.

However, the polydispersity index (PDI) indicated the degree of monodispersity of a nanoparticle system and the size of the nanoparticles. The PDI values obtained were 0.403, 0.456, and 0.579, respectively. If the PDI value was lower, it was better to distribute the particle size, as this reflected the size distribution of the nanoparticles dispersed within the gold-containing colloidal particles. Therefore, an PDI value close to zero indicated a homogeneous dispersion, and an PDI value greater than 0.5 indicated high heterogeneity (Avadi et al., 2010).

The increase in PI value with increasing extract concentration suggests that excessive red ginger rhizome extract may promote broader particle size distribution. This may occur because higher concentrations of phytochemicals can accelerate Au^{3+} reduction and particle growth, while excess organic compounds may also form non-uniform capping layers or promote interparticle association. Therefore, the PI trend supports the PSA/DLS particle size results, indicating that higher extract concentrations did not improve nanoparticle uniformity but instead produced a more heterogeneous colloidal system.

Although the UV-Vis spectra showed absorption bands in the surface plasmon resonance region of gold nanoparticles, this evidence alone is not sufficient to conclusively confirm the morphology, actual core size, crystallinity, and surface chemistry of the particles. PSA/DLS provides hydrodynamic diameter, which may include the gold core, phytochemical capping layer, CMC-Na polymer coating, solvation layer, and possible aggregates. Therefore, the particle sizes reported in this study should not be directly interpreted as the metallic core size of individual AuNPs. TEM analysis is required to observe the actual morphology, core size, and particle distribution, while FTIR analysis is needed to identify functional group changes associated with Au^{3+} reduction, phytochemical capping, and CMC-Na interaction. XRD and EDX/EDS analyses would also strengthen the confirmation of crystalline metallic gold and elemental composition.

The variation in extract concentration influenced the hydrodynamic size of the formed particles. The smallest particle size was obtained at 600 ppm, while higher extract concentrations of 900 and 1200 ppm produced larger hydrodynamic diameters. This result suggests that increasing the extract concentration did not necessarily improve particle size control. A higher amount of organic compounds in the extract may accelerate the reduction process and provide more capping molecules; however, excessive phytochemical content may also increase the organic layer around the particles and promote interparticle interactions, leading to larger hydrodynamic sizes and broader size distributions. Therefore, 600 ppm was selected as the most appropriate concentration among the tested formulations for further stabilization

using CMC-Na. Nevertheless, this selection was based on preliminary screening, and further optimization using a systematic experimental design is required to determine the optimum synthesis conditions.

Furthermore, characterization using a polarizing microscope was performed as a preliminary qualitative observation to assess whether particulate structures were present in the dried gold-containing colloidal sample after 24 h. The observation suggested the presence of particulate domains and possible micro-scale aggregates within the dried film. However, because the spatial resolution of optical microscopy is limited to the micrometer scale, individual gold nanoparticles could not be directly visualized, and the technique was not used to determine particle size or morphology. Therefore, the polarizing microscopy results were considered only as supportive qualitative evidence of particle formation, whereas detailed characterization of nanoparticle morphology and size distribution requires higher-resolution techniques such as TEM.

In the formation of gold nanoparticles, three concentrations of the CMC-Na stabilizer were used sequentially: 0.5%, 1%, and 2%. Gold-containing colloidal particles with CMC-Na concentrations of 0.5 and 1% were checked at H0 or at the 1st hour after being checked using PSA (Fig. 5). It turned out that larger clusters had formed, with sizes of 1451.6 nm and 1336.93 nm, respectively. In this case, the sizes were no longer within the nanoscale range. This is thought to be because the concentration of the added stabilizer was insufficient to form large clusters. However, for a concentration of 2% at H0 or at the 1st hour, nanoparticles with a size of 984.03 nm had been formed.

The relatively better performance of 2% CMC-Na compared with 0.5% and 1% CMC-Na may be related to its ability to provide stronger steric and electrostatic stabilization. CMC-Na contains carboxylate groups that can contribute to negative surface charge and electrostatic repulsion between particles, while its polymer chains can create steric barriers that reduce direct particle-particle contact. At lower concentrations, CMC-Na may not sufficiently cover the particle surface, allowing particles to collide and aggregate more easily. In contrast, 2% CMC-Na may provide more extensive surface coverage and a thicker protective layer, thereby delaying aggregation. However, excessive or non-uniform polymer adsorption may also lead to polymer bridging between particles, which explains why large hydrodynamic sizes were still observed and why long-term stability was not achieved.

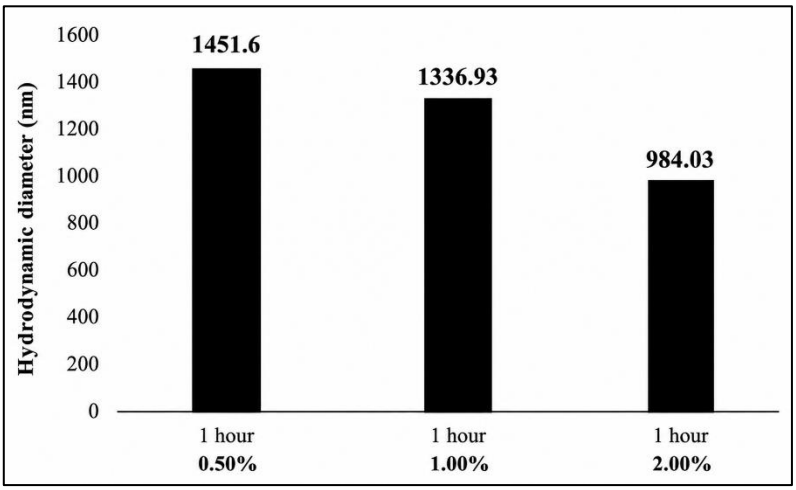

Figure 4. Hydrodynamic Particle Size of Gold-Containing Colloidal Systems After 1 H with Different CMC-Na Concentrations

The stability test (Table 4) showed that 2% CMC-Na delayed particle aggregation only for a limited period. The initial decrease in hydrodynamic diameter from 984.03 nm at 60 minutes to 769.53 nm at 20 h and 599.4 nm at 7 days may be associated with polymer-layer rearrangement, redistribution of loosely bound aggregates, and temporary stabilization of smaller colloidal domains by CMC-Na. However, the subsequent increase to 864.93 nm on day 14 and 1,051.03 nm on day 21 indicates progressive aggregation. This behavior may be explained by aggregation kinetics, polymer bridging, and possible Ostwald ripening. The high PDI value on day 21 further supports the formation of a highly heterogeneous and aggregated colloidal system.

It should be noted that the particle size measured by PSA represents the hydrodynamic diameter rather than the actual metallic gold core size. The hydrodynamic diameter may include the AuNP core, phytochemical compounds adsorbed from red ginger rhizome extract, CMC-Na polymer layers, solvation layers, and possible interparticle aggregates. Therefore, the relatively large particle sizes observed after CMC-Na addition, ranging from approximately 599.4 to 984.03 nm during 14 days of storage, indicate that the colloidal system was not composed of well-dispersed small AuNPs but rather of polymer-coated and/or aggregated AuNP structures.

The increase in particle size after CMC-Na addition may be attributed to the interaction between CMC-Na chains and the surface of phytochemical-capped AuNPs. At relatively high polymer concentration, CMC-Na may increase the viscosity of the dispersion medium and induce bridging flocculation, in which one polymer chain interacts with several particles simultaneously. This phenomenon can promote the formation of larger colloidal aggregates instead of preventing aggregation. Therefore, although 2% CMC-Na showed better stability than 0.5% and 1% CMC-Na, the resulting particles cannot yet be considered well-dispersed AuNPs suitable for biomedical applications.

Furthermore, zeta potential measurements were performed to characterize the nanoparticles' surface charge properties and electrostatic interactions. This interaction determined a nanoparticle's tendency to aggregate (Abdassah et al., 2009). The colloidal dispersion was considered stable when the zeta potential was greater than +30 mV or less than −30 mV (Honary & Zahir, 2013).

Table 5. Storage Stability of The 2% CMC-Na-Stabilized Gold Colloidal System

Time	dH (nm)	PDI	Zeta potential (mV)
60 minutes	984.03	0.66	-110.97
20 hours	769.53	0.47	-152.83
7 days	599.4	0.55	-65.47
14 days	864.93	0.72	-56.27
21 days	1,051.03	1.289	-

Note: dH = hydrodynamic diameter

Based on Table 5, the 2% CMC-Na formulation showed highly negative zeta potential values from 60 minutes to 14 days, suggesting the presence of negatively charged colloidal particles, possibly due to adsorption of anionic CMC-Na on the particle surface. In Table 5, dH refers to hydrodynamic diameter. However, these values should be interpreted cautiously because the extremely negative values may be affected by polymer concentration, pH, ionic strength, dilution, and measurement conditions. Moreover, the large hydrodynamic particle size and increased PDI indicate that the

system still underwent aggregation despite its negative surface charge.

A limitation of the present study is that not all characterization data were obtained from independent replicate syntheses. Therefore, some particle size, PDI, and zeta potential data are presented descriptively without statistical significance testing. As a consequence, the observed differences among formulations should be interpreted as preliminary trends rather than statistically confirmed differences. Future studies should include independent synthesis replicates, report all quantitative data as mean ± SD, and apply appropriate statistical analysis to evaluate the significance of formulation effects on particle size, PDI, zeta potential, and colloidal stability.

4. Conclusion

Red ginger rhizome extract showed potential as a bioreducing agent for the formation of gold-containing colloidal particles, as indicated by the color change and UV-Vis absorption bands in the surface plasmon resonance region. The initial particle sizes obtained without CMC-Na were 137 nm, 208.4 nm, and 233.4 nm for extract concentrations of 600, 900, and 1200 ppm, respectively. However, after the addition of CMC-Na, the measured hydrodynamic diameters increased substantially, indicating the formation of polymer-coated and/or aggregated colloidal structures. Among the tested stabilizer concentrations, 2% CMC-Na showed relatively better colloidal stability up to 14 days. However, this formulation did not provide long-term colloidal stability. The resulting particle sizes remained larger than the ideal size range commonly expected for well-dispersed AuNPs in biomedical applications. Therefore, further optimization, additional characterization, and appropriate statistical analysis are required to obtain smaller, more uniform, and stable AuNPs.

References

Abdassah, M., Rusdiana, T., Subghan, A., & Hidayati, G. (2009). Formulasi Gel Pengelupas Kulit Mati yang Mengandung Etil Vitamin C dalam Sistem Penghantaran MacrobeadÂ®. *Jurnal Ilmu Kefarmasian Indonesia*, *7*(2), 105-111. Retrieved from https://jifi.farmasi.univpancasila.ac.id/

Aditya, M., & Ariyanti, P. R. (2016). Manfaat gambir (Uncaria gambir Roxb) sebagai antioksidan. *Majority*, *5*(3), 129-133. Retrieved from https://juke.kedokteran.unila.ac.id/index.php/majority

Amiruddin, M. A., & Taufikurrohmah, T. (2013). Synthesis and characterization of gold nanoparticles using a matrix of bentonite in scavenging free radicals in cosmetics. *UNESA Journal of Chemistry Vol*, *2*, 68-75. Retrieved from https://journal.unesa.ac.id/index.php/unesa-journal-of-chemistry

Avadi, M. R., Sadeghi, A. M. M., Mohammadpour, N., Abedin, S., Atyabi, F., Dinarvand, R., & Rafiee-Tehrani, M. (2010). *Preparation and characterization of insulin nanoparticles using chitosan and Arabic gum with ionic gelation method*. Nanomedicine: Nanotechnology, Biology and Medicine, 6(1), 58–63. https://doi.org/10.1016/j.nano.2009.04.007

Bharadwaj, K. K., Rabha, B., Pati, S., Sarkar, T., Choudhury, B. K., Barman, A., ... & Mohd Noor, N. H. (2021). Green synthesis of gold nanoparticles using plant extracts as beneficial prospect for cancer theranostics. *Molecules*, *26*(21), 6389. https://doi.org/10.3390/molecules26216389

DeFrates, K., Markiewicz, T., Gallo, P., Rack, A., Weyhmiller, A., Jarmusik, B., & Hu, X. (2018). Protein polymer-based nanoparticles: fabrication and medical applications. *International journal of molecular sciences*, *19*(6), 1717. https://doi.org/10.3390/ijms19061717

Dewi, N. W. R. K., Yasa, G. T., & Santi, M. D. S. (2024). Potensi ekstrak etanol 96% rimpang jahe merah (Zingiber officinale var. rubrum) sebagai antioksidan. *Jurnal Skala Husada: The Journal of Health*, *21*(2), 57-62. Retrieved from https://ejournal.poltekkes-denpasar.ac.id

Elia, P., Zach, R., Hazan, S., Kolusheva, S., Porat, Z., & Zeiri, Y. (2014). *Green synthesis of gold nanoparticles using plant extracts as reducing agents*. *International Journal of Nanomedicine, 9*, 4007–4021. https://doi.org/10.2147/IJN.S57343

Evans, W. C. (2009). *Trease and Evans Pharmacognosy* (16th ed.). Saunders Elsevier.

Fabiani, V. A., Sutanti, F., Silvia, D., & Putri, M. A. (2018). Green synthesis nanopartikel perak menggunakan ekstrak daun pucuk idat (Cratoxylum glaucum) sebagai bioreduktor. *Indonesian Journal of Pure and Applied Chemistry*, *1*(2), 68-76. Retrieved from https://journal.ubb.ac.id/index.php/ijpac

Farnsworth, N. R. (1966). Biological and phytochemical screening of plants. *Journal of pharmaceutical sciences*, *55*(3), 225-276. https://doi.org/10.1002/jps.2600550302

Fouda, A., Eid, A. M., Guibal, E., Hamza, M. F., Hassan, S. E. D., Alkhalifah, D. H. M., & El-Hossary, D. (2022). Green synthesis of gold nanoparticles by aqueous extract of Zingiber officinale: characterization and insight into antimicrobial, antioxidant, and in vitro cytotoxic activities. *Applied Sciences*, *12*(24), 12879. https://doi.org/10.3390/app122412879

Harborne, J. B. (1987). Metode fitokimia K. Padmawinata & I. Soediro, Trans.). *ITB*

Harborne, J. B. (1998). *Phytochemical Methods: A Guide to Modern Techniques of Plant Analysis* (3rd ed.). Chapman & Hall.

Hebeish, A. A., El-Rafie, M. H., Abdel-Mohdy, F. A., Abdel-Halim, E. S., & Emam, H. E. (2010). Carboxymethyl cellulose for green synthesis and stabilization of silver nanoparticles. *Carbohydrate polymers*, *82*(3), 933-941. https://doi.org/10.1016/j.carbpol.2010.06.020

Honary, S., & Zahir, F. (2013). *Effect of zeta potential on the properties of nano-drug delivery systems – A review (Part 1).* Tropical Journal of Pharmaceutical Research, 12(2), 255–264. https://doi.org/10.4314/tjpr.v12i2.19

Huq, M. A., Rana, M. R., Samad, A., Rahman, M. S., Rahman, M. M., Ashrafudoulla, M., ... & Park, J. W. (2025). Green synthesis, characterization, and potential antibacterial and anticancer applications of gold nanoparticles: current status and future prospects. *Biomedicines*, *13*(5), 1184. https://doi.org/10.3390/biomedicines13051184

Jain, P. K., Huang, X., El-Sayed, I. H., & El-Sayed, M. A. (2006). *Gold nanostructures: Engineering their plasmonic properties for biomedical applications*. Chemical Society Reviews, 36(11), 1744–1755. https://doi.org/10.1039/B615786B

Kamaluddin, I. D. K., Nawawi, N. M., Syamsu, R. F., Royani, I., & Bima, I. H. (2024). Comparison of Antioxidants in Red Ginger Powder Preparations without the addition of sucrose. *Poltekita: Jurnal Ilmu Kesehatan*, *17*(4), 1436-1441. https://doi.org/10.33860/jik.v17i4.3554

Khairun, N. B., & Desty, M. (2018). Efektivitas kulit batang bakau minyak (Rhizopora apiculata) sebagai antioksidan. *Jurnal Agromedicine*, *5*(1), 412-417. Retrieved from http://repository.lppm.unila.ac.id/8939/

Khairurrijal, K., & Abdullah, M. (2009). Review: Karakterisasi Nanomaterial. *Jurnal Nanosains & Nanoteknologi*, *2*(1), 1-8. Retrieved from https://www.researchgate.net/publication/26844441_Review_Karakterisasi_Nanomaterial

Lembang, E. Y. (2013). *Sintesis nanopartikel perak dengan metode reduksi menggunakan bioreduktor ekstrak daun ketapang (terminalia catappa)* (Doctoral dissertation, Universitas Hasanuddin). Retrieved from https://repository.unhas.ac.id/id/eprint/8886/1/estyyunita-1387-1-13-esty-g%201-2.pdf

Molyneux, P. (2004). The use of the stable free radical diphenylpicrylhydrazyl (DPPH) for estimating antioxidant activity. *Songklanakarin Journal of Science and Technology, 26*(2), 211–219. Retrieved from https://d1wqtxts1xzle7.cloudfront.net/39013361/Molineux_07-DPPH-libre.pdf

Muddapur, U. M., Alshehri, S., Ghoneim, M. M., Mahnashi, M. H., Alshahrani, M. A., Khan, A. A., ... & Ahmad, M. Z. (2022). Plant-based synthesis of gold nanoparticles and theranostic applications: a review. *Molecules*, *27*(4), 1391. https://doi.org/10.3390/molecules27041391

Munadi, R. (2020). Analisis komponen kimia dan uji aktivitas antioksidan ekstrak rimpang jahe merah (Zingiber officinale Rosc. Var Rubrum). *Cokroaminoto Journal of Chemical Science*, *2*(1), 1-6. Retrieved from https://science.e-journal.my.id/cjcs/article/view/31

Nisha, Sachan, R. S. K., Singh, A., Karnwal, A., Shidiki, A., & Kumar, G. (2024). Plant-mediated gold nanoparticles in cancer therapy: Exploring anti-cancer mechanisms, drug delivery applications, and future prospects. *Frontiers in nanotechnology*, *6*, 1490980. https://doi.org/10.3389/fnano.2024.1490980

Nuraeni, W., Daruwati, I., Widyasari, E. M., & Sriyani, M. E. (2013). Verifikasi kinerja alat Particle Size Analyzer (PSA) HORIBA LB-550 untuk penentuan distribusi ukuran nanopartikel. Prosiding Seminar Nasional Sains dan Teknologi Nuklir, Bandung, Indonesia, 4 Juli 2013, 266–271. PTNBR–BATAN. Retrieved from https://d1wqtxts1xzle7.cloudfront.net/78428584/09_KK_38_Witri_20Nuraeni_ptnbr_266-271-libre.pdf

Santhosh, P. B., Genova, J., & Chamati, H. (2022). Green synthesis of gold nanoparticles: An eco-friendly approach. *Chemistry*, *4*(2), 345-369. https://doi.org/10.3390/chemistry4020026

Shankar, S. S., Rai, A., Ahmad, A., & Sastry, M. (2004). Rapid synthesis of Au, Ag, and bimetallic Au core–Ag shell nanoparticles using neem (Azadirachta indica) leaf broth. *Journal of Colloid and Interface Science, 275*(2), 496–502. https://doi.org/10.1016/j.jcis.2004.03.003

Singh, G., Kapoor, I. P. S., Singh, P., de Heluani, C. S., de Lampasona, M. P., & Catalan, C. A. (2008). Chemistry, antioxidant and antimicrobial investigations on essential oil and oleoresins of Zingiber officinale. *Food and chemical toxicology*, *46*(10), 3295-3302. https://doi.org/10.1016/j.fct.2008.07.017

Tadros, T. F. (2007). General principles of colloid stability and the role of surface forces. In T. F. Tadros (Ed.), *Colloid stability: The role of surface forces* (Vol. 1, pp. 1–22). Wiley-VCH Verlag GmbH & Co. KGaA.

https://doi.org/10.1002/9783527631070.ch1

Tarhan, T., Tural, B., & Tural, S. (2019). Synthesis and characterization of new branched magnetic nanocomposite for loading and release of topotecan anti-cancer drug. *Journal of Analytical Science and Technology*, *10*(1), 30. Retrieved from https://link.springer.com/article/10.1186/s40543-019-0189-x

Taufikurohmah, T., Sanjaya, I. G. M., Baktir, A., & Syahrani, A. (2012). Activity test of nanogold for reduction of free radicals, a pre-assessment utilization nanogold in pharmaceutical as medicines and cosmetics. *J. Mater. Sci. Eng. B*, *2*(12), 611-617. Retrieved from https://www.researchgate.net/publication/235725713_Journal_of_Materials_Science_and_Engineering

Tetti, M. (2014). Ekstraksi, pemisahan senyawa, dan identifikasi senyawa aktif. *Jurnal Kesehatan*, *7*(2). https://doi.org/10.24252/kesehatan.v7i2.55

Thakkar, K. N., Mhatre, S. S., & Parikh, R. Y. (2010). Biological synthesis of metallic nanoparticles. *Nanomedicine: nanotechnology, biology and medicine*, *6*(2), 257-262. https://doi.org/10.1016/j.nano.2009.07.002

Villagrán, Z., Anaya-Esparza, L. M., Velázquez-Carriles, C. A., Silva-Jara, J. M., Ruvalcaba-Gómez, J. M., Aurora-Vigo, E. F., Rodríguez-Lafitte, E., Rodríguez-Barajas, N., Balderas-León, I., & Martínez-Esquivias, F. (2024). *Plant-Based Extracts as Reducing, Capping, and Stabilizing Agents for the Green Synthesis of Inorganic Nanoparticles*. Resources, 13(6), 70. https://doi.org/10.3390/resources13060070

Wahyudi, T., Sugiyana, D., & Helmy, Q. (2011). Sintesis nanopartikel perak dan uji aktivitasnya terhadap bakteri E. coli dan S. aureus. *Arena Tekstil*, *26*(1). https://doi.org/10.31266/at.v26i1.1442

World Health Organization. (2011). *Quality Control Methods for Herbal Materials*. Geneva: World Health Organization.

Yuliani, N. N., Sambara, J., & Mau, M. A. (2016). Uji aktivitas antioksidan fraksi etilasetat ekstrak etanol rimpang jahe merah (Zingiber officinale var. rubrum) dengan metode DPPH (1, 1-diphenyl-2-picrylhydrazyl). *Jurnal Info Kesehatan*, *14*(1), 1091-1111. Retrieved from https://media.neliti.com/media/publications/259692-test-activities-antioxide-etilasetat-fra-edf1501b.pdf